Correlations in a one-dimensional lattice fluid on Si(111)5×2-Au

A. Kirakosian, R. Bennewitz,* F.J. Himpsel, and L.W. Bruch
Department of Physics, University of Wisconsin–Madison, Madison, Wisconsin 53706
(Received 10 December 2002; published 16 May 2003)

The Si(111)5×2 Au surface forms a chain structure with a quarter-filled lattice fluid of additional Si atoms on top of the chains. The pair distribution function $g(r)$ of these extra atoms is determined from an extensive set of scanning tunneling microscopy data covering (~4500 adatoms) and is used to estimate the adatom-adatom interactions. A small probability of simultaneous occupation of nearest-neighbor sites reflects a repulsion of 220 meV ($3.6k_BT$). Persistent oscillations in $g(r)$ are fit by a periodic potential of amplitude 1.2 meV ($0.02k_BT$), which might arise from an incipient charge density wave. The interchain correlations are very small. A good fit is obtained by a repulsive energy between interchain nearest neighbors of less than 12 meV ($0.2k_BT$), demonstrating the one-dimensional character of the lattice fluid. In addition to providing microscopic data on a one-dimensional lattice fluid the results help explain the limits of data storage density due to interactions between adjacent bits.

DOI: 10.1103/PhysRevB.67.205412 PACS number(s): 68.37.Ef; 68.65.−k; 05.50.+q

I. INTRODUCTION

One of the motivations for studying physics in lower dimensions is that properties of three-dimensional extended phases should change in a systematic fashion when the degrees of freedom are constrained. The modeling becomes more tractable and more explicit for the lower-dimensional cases. One-dimensional systems are an extreme case of such considerations. Structures with essentially one-dimensional correlations are realized with highly anisotropic magnetic salts[1] and with adsorption at nanotubes or nanotube bundles.[2,3] The present work considers chains of adatoms at a silicon surface as a well-controlled example of nearly one-dimensional (1D) correlations.

Previous work[4] has demonstrated one-dimensional diffusion along the chains. Our study finds that the interaction energy between the closest adatoms in neighboring chains is at least 10 times smaller than that along the chains, so small that it falls close to the detection limit. The nature of the experimental information is qualitatively different from that available for other 1D systems. The spatial correlation function is obtained directly from the analysis of the scanning tunneling microscopy (STM) images, while for the other systems, the information is mostly for the equation of state. The silicon adatoms occupy discrete sites of the surface lattice, but they have a strong short-range repulsion. Thus the corresponding lattice gas has low probability for occupation of nearest-neighbor sites and the model is analogous to that for an antiferromagnetic Ising chain. The quarter-filled lattice corresponds to a high applied magnetic field case, which has been studied in experiments on the quasi-one-dimensional Ising antiferromagnet[5] $CsCoCl_3$.

There are a variety of silicon surfaces that form one-dimensional chain structures when metal atoms are adsorbed at submonolayer coverage.[6] On Si(111), such chain structures develop at stepped surfaces or even on flat Si(111) by spontaneous breaking of the threefold symmetry into three domains with an angle of 120° between the chains. These chains are formed by alkali metals, alkaline earths, noble metals, and even magnetic rare earths, as long as the coverage is well below one monolayer. The Si(111)5×2 Au structure, for example, contains 0.4 monolayer of Au which corresponds to two gold chains per unit cell.[4,7–14] It is surprising that the threefold symmetry of Si(111) is broken in all these chain structures. Their stability might be related to the stability of the honeycomb chain (HCC),[15] which is a structural element in many of them. This chain consists of a strip of graphitic, π-bonded Si. The detailed structure of Si(111)5×2 Au is still uncertain, although a number of structural studies have led to specific models.[4,10–12,14]

Some of the chain structures exhibit additional atoms on top of the chains, such as Si(557) Au with 1/100 monolayer and Si(111)5×2 Au with 1/40 monolayer.[16] The latter has been studied in detail,[4,11,13,17] and it has been found that the extra atoms reside on a 5×2 lattice, but occupy only a quarter of the available sites [1/40 of a monolayer; see Fig. 1(a)]. After lingering uncertainty about whether the extra atoms are Si or Au it has been demonstrated that empty sites can be filled by depositing 1/40 of a monolayer of additional Si; i.e., the adatoms are[18,19] Si. The resulting half-filled 5×2 lattice is only metastable and converts to the quarter-filled 5×2 lattice above 300 °C, with excess Si moving to the nearest step. The quarter-filled lattice of Si adatoms has been used to demonstrate an atomic-scale memory, where a bit is represented by the presence or absence of a Si adatom.[18] This memory has served as a test bed for investigating fundamental limits of data storage, such as density, data rate, retention, and signal to noise. The density, in particular, lies right at the fundamental limit where interactions between neighbor atoms cause correlations between adjacent bits. For example, a bit separation of two Si(111) lattice constants ($2a_{Si}=7.68$ Å) is 30 times less likely to occur than the next closest bit separation of $4a_{Si}$, which would make a memory with twice the density unrealistic at this surface. The cell size of a quarter-filled adatom lattice is very similar to the bit size of 5×5×5 atoms taken by Feynman in his groundbreaking 1959 talk[20] for illustrating the consequences of an atomic-scale memory. Actually, nature needs 32 atoms to store 1 bit in DNA using half of a base pair. Such comparisons bring up the broader question of the smallest possible bit size in a memory, which

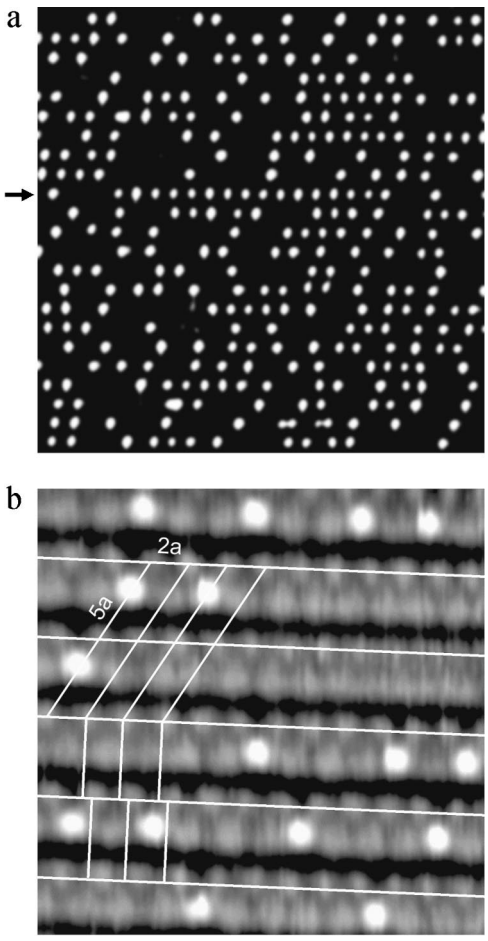

FIG. 1. STM images of the Si(111)5×2 Au surface showing a pair of atomic chains in (b) and extra Si atoms on top of the chains (bright dots). The Si adatoms are enhanced in (a) by resonant tunneling at −2 V sample bias [versus −1.5 V in (b)] and by an increased contrast. Two 5×2 grids are outlined in (b). The frame size is 38×38 nm^2 in (a) and 9×9 nm^2 in (b).

is largely determined by correlations between adjacent bits.

In this study we determine the correlations between the extra atoms on top of the Si(111)5×2 Au surface and infer the underlying interaction potential. There have been previous studies of this system involving Monte Carlo simulations,[17] but the data sets were less complete and the surface defect density was higher. After testing a variety of interaction models we find that two ingredients are required to reproduce the observed pair correlation function: (1) a strong nearest-neighbor repulsion and (2) a long-range, oscillatory interaction that is reminiscent of the pinning of $c(4\times2)$ ordering on Si(100)2×1 near defects.

II. EXPERIMENT

Vicinal Si(111) surfaces tilted by 1° towards the $[\overline{112}]$ azimuth are used as substrates. By applying a previously optimized annealing sequence,[21] a regular pattern of straight steps with large domains of the 7×7 reconstruction is obtained. The use of a slightly stepped Si(111) substrate stabilizes one of the three possible Si(111)5×2 Au domain orientations.[22] Gold is evaporated from a molybdenum wire basket with a typical rate of 0.015 monolayers per second with the sample held at a temperature of 650 °C. Subsequently, the sample is annealed to 950 °C. The sample can then be repeatedly cleaned by annealing to 850 °C. The coverage is calibrated using low-energy electron diffraction (LEED) and STM. At Au coverage below the optimum, patches of Si(111)7×7 coexist with the 5×2 Au structure, while patches of the Au-rich $\sqrt{3}\times\sqrt{3}$ Au structure appear when the coverage is too high.[19] All STM images are recorded *in situ* at room temperature. An example of the STM data is shown in Fig. 1, where the bright protrusions correspond to extra Si atoms on top of the chains.

In order to explore the role of defects at nonstoichiometric surfaces, i.e., gold coverage not equal to 0.4 monolayer, we analyze two sets of data, one near optimum coverage and the other with excess Au. Although the coverage of Si adatoms is rather stable with respect to Au coverage, it eventually drops with a large amount of extra Au. The stoichiometric data set contains a total of 3094 Si adatoms spread over 12 468 sites of the 5×2 lattice with a coverage of 0.248 ± 0.004. The Au-rich data set contains a total of 1359 Si atoms over 7260 sites of the 5×2 lattice at a coverage of 0.187 ± 0.005. Distinct correlation functions are obtained, as shown in Fig. 2. Calculation of the pair distribution function $g(r)$ from STM images involves periodic boundary conditions, so atoms at the edges of the image are included in the counting. This procedure has very little effect on the pair distribution function for small distances ($r<15a_{Si}$). The changes are less than 1% compared to the calculation of $g(r)$ with fixed boundary conditions when adatoms at the image edge have neighbors only on one side. The effect is somewhat greater for larger distances (1%—3% for $15a_{Si}<r<40a_{Si}$) because of the finite image sizes. The use of periodic boundary conditions improves the statistics.

III. PAIR DISTRIBUTION FUNCTION FROM STM IMAGES

Typical STM images of the Si(111)5×2 Au surface are shown in Fig. 1. There are two distinct features of the surface, bright dots and a pair of underlying chains [suppressed by high contrast in Fig. 1(a)]. The bright protrusions correspond to extra Si atoms adsorbed on top of the chains. They can be highlighted by resonant tunneling at a sample bias of −2 eV [Fig. 1(a)], indicating a characteristic occupied state at 2 eV below the Fermi level. The Si adatoms form a lattice fluid that is frozen in at room temperature and becomes mobile above about 500 K according to previous high-temperature STM studies.[4] Following the choice of Hasegawa and Hosoki[4] and Yagi *et al.*[17] we assume that the system still maintains thermal equilibrium down to 700 K and this sets the energy scale for the interactions in the modeling.

The lattice underlying the extra Si atoms has a periodicity of five Si(111) lattice constants between the rows $[5a_{Si}\cos(30°)=16.63$ Å] and two lattice constants along the

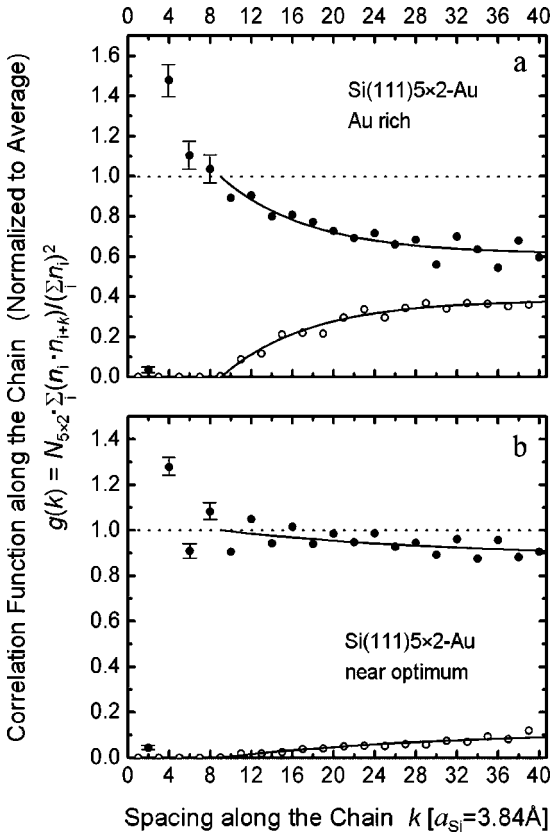

FIG. 2. The correlation function between Si adatoms along the chain obtained from STM images with excess coverage of Au (a) and near-optimum coverage (b). $N_{5\times2}$ is the total number of 5×2 sites and $n_i=0$, 1 is the occupation number of site i. Solid circles represent the even-numbered separations, open circles the odd-numbered separations induced by 5×2 domain boundaries. The nearest-neighbor site ($k=2$) is strongly suppressed by a repulsive interaction.

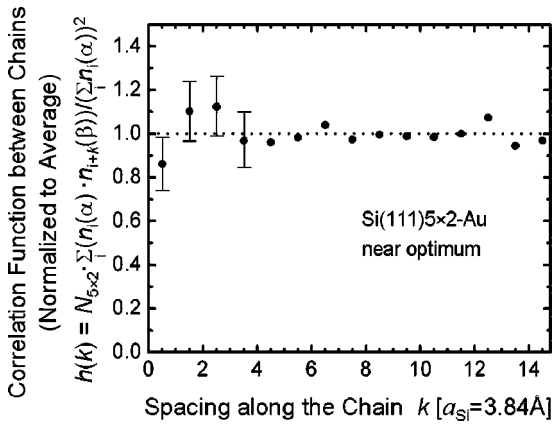

FIG. 3. Experimental correlation function between Si atoms in adjacent chains α and β showing weak interchain coupling with a slight repulsion of nearest neighbors. Data points are defined only for half-integer values of k due to the offset in the rectangular unit cells [see Fig. 1(b)].

rows. Two different unit cells of the 5×2 structure are overlaid in white in Fig. 1(b), one based on the triangular lattice of the Si(111) surface and the other displaying the rectangular cell used for the modeling in Sec. IV. When moving from one row to the next the rectangular cell is shifted by $\pm\frac{1}{4}$, which corresponds to $\pm\frac{1}{2}$ of the Si(111) lattice constant along the chains ($a_{Si}=3.84$ Å). This shift breaks the mirror symmetry about the (1 1 0) plane and creates two mirror domains with equal probability. As a result, the correlation function between adjacent chains in Fig. 3 is defined for the half-integer separations (i.e., $\frac{1}{2}a_{Si}, \frac{3}{2}a_{Si}, \ldots,$ etc.), whereas the correlation along the same chain in Fig. 2 is for integer separations only.

The Si adatoms which are the subject of this study occur only on a specific site of the 5×2 unit cell [see Fig. 1(b) and high-resolution images in Ref. 11]. The fact that adatoms along a row are also observed at separations containing an odd number of a_{Si} indicates that the underlying 5×2 lattice between these adatoms must have slipped by $1a_{Si}$ relative to the Si(111)1×1 bulk lattice. The point where the slip occurs corresponds to a domain boundary and the stretches of slip-free 5×2 rows to single domains. These are particularly large in our study of stoichiometric surfaces, and this enables us to extract the intrinsic behavior of a single domain.

The correlation function $g(k)$ between extra Si atoms along a chain is plotted in Fig. 2(a) for a gold-rich surface and for the stoichiometric gold coverage, Fig. 2(b). The unit k along the x axis corresponds to a Si(111)1×1 lattice constant a_{Si}, i.e., half of the lattice spacing of the 5×2 surface which is used as the unit in the lattice gas model in Sec. IV. The function $g(k)$ is symmetric $g(k)=\frac{1}{2}[g(k)+g(-k)]$. We immediately identify two common features to the data in (a) and (b): the absence of odd-numbered separations (open circles) for $k<10$ and a very small probability [3.5% and 4.3% of the average value for (a) and (b), respectively] for the first even-numbered separation $k=2$. As explained in the following, the odd separations correspond to defects created by domain boundaries, and the nearest even separation is suppressed by strong nearest-neighbor repulsion.

The odd-numbered 5×1 lattice separations $k=1,3,5,7,9$ are empty, as expected for a perfect 5×2 lattice. Higher odd-numbered separations gradually become populated due to the occurrence of domain boundaries between the two 5×2 domains that are shifted by a_{Si} along the rows. (Domains shifted perpendicular to the chains are so rare in our data that they can be neglected.) The domain walls occur more frequently for the Au-rich surface [compare the open circles in Figs. 2(a) and 2(b)]. This is not surprising because the incorrect stoichiometry should lead to a high density of defects that can pin domain walls. For comparison, the occupancy of odd-numbered separations in previous work[17] was about 4 times larger than in Fig. 2(b) and 1.5 times smaller than in Fig. 2(a). A simple exponential fit in a form $y_0-y_1\exp(-k/k_0)$ describes the occurrence of odd-numbered separations rather well, as shown by the lines through open circles in Fig. 2. Subtracting the same exponential from the average value of 1 (dashed line in Fig. 2) produces a close fit to the decaying number of even-numbered separations (solid dots). Such a close match indicates that the missing even-numbered entries are due to the formation of multiple domains along the chains.[23] For normalization we divide the raw pair distri-

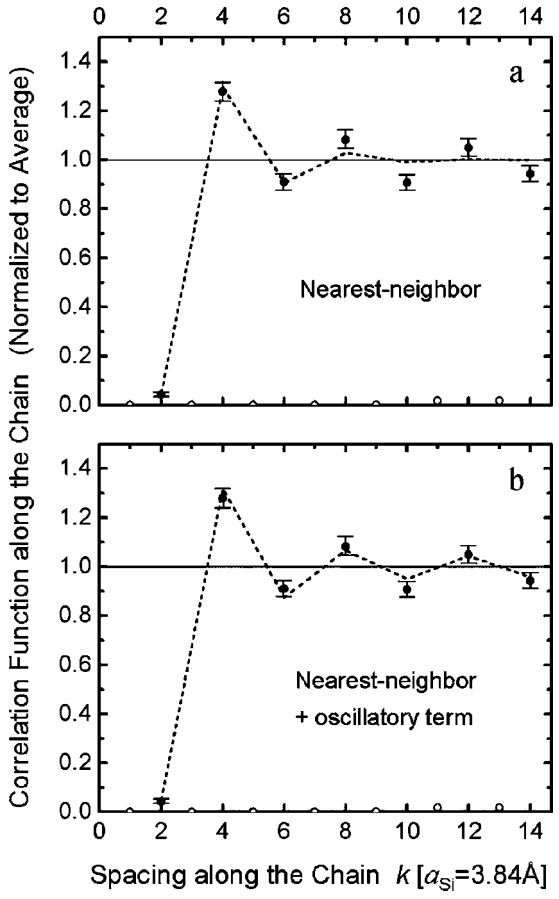

FIG. 4. Comparison of the experimental correlation function along the chains (circles) with the result from two models (dashed lines). Nearest-neighbor repulsion alone can describe the suppression at the $k=2$ separation and the resulting pileup at $k=4$ (a), but an extra oscillatory interaction is required to explain the subsequent oscillations for $k>6$ (b).

bution function, the total number of pairs at separation k, by the random number of pairs $N_R=N_{5\times2}\langle n_i\rangle^2$, where $N_{5\times2}$ is the total number of 5×2 sites and $\langle n_i\rangle$ is the average density. For the Au-rich surface in Fig. 2(a), $N_R=7260\times(0.187)^2=254$ and parameter values for the fits are $y_0=0.369$, $y_1=1.147$, and $k_0=8.59$. For the stoichiometric surface in Fig. 2(b) the values are $N_R=12\,468\times(0.248)^2=767$, $y_0=0.119$, $y_1=0.178$, and $k_0=22.60$. The comparison with theory for $g(k)$ in Fig. 4 covers only the low-k region where the effect of domain boundaries is negligible.

The effect of short-range repulsion can be seen clearly from the low probability of only 3.5% and 4.3% for the smallest allowed separation $2a_{Si}$ [Figs. 2(a) and 2(b), respectively], normalized to the random probability for the number of pairs at separation k. This can be seen already from Fig. 1(a), where the occurrence of two Si adatoms separated by $2a_{Si}$ is very rare. Two such objects can be seen near the middle of the second row from the bottom.

A consequence of the highly suppressed $k=2$ separation is that there is a pile up of the displaced atoms at the next even-numbered separation $k=4$. This feature is common to the correlation functions for both surfaces in Fig. 2. An alternative explanation of the peak by an attractive interaction for $k=4$ is excluded by explicit modeling described in Sec. V.

The $g(k)$ in Fig. 2(b) (stoichiometric surface) has an oscillatory behavior that persists for values of k higher than 6. As discussed in Sec. V, this behavior is indicative of a long-range interaction along the one-dimensional chains. The presence of a large number of defects on the Au-rich surface destroys these correlations and gives rise to a monotonic decay of the correlation function in Fig. 2(a). The correlation function drops much below the random average of 1 and for large k is approaching the asymptotic value[23] 0.5.

In order to complete the survey of interatomic interactions on the Si(111)5×2 Au we plot the correlation function $h(k)$ between adjacent chains in Fig. 3. As explained at the beginning of this section, $h(k)$ is defined for half-integer values of k due to the offset between the rectangular unit cells that are used to define the correlation function [Fig. 1(b)]. All values of the $h(k)$ in Fig. 3 lie very close to the random average value, indicating that the correlation across the chains is weak. In fact, the average value shown as a dotted line lies within the statistical error bars for all the points with the exception of the first one ($k=\frac{1}{2}$). The occupation of nearest-neighbor sites in adjacent chains appears to be slightly suppressed by a weak repulsion, which we estimate in Sec. V by using the model Hamiltonian H^{II} defined in Eq. (3).

The dotted line in Fig. 3 again represents the random occupation of pairs of sites, which is defined the same way as for $g(k)$ in Fig. 2. We find that within statistical uncertainty a shift of $\frac{1}{2}a_{Si}$ (to the right) is as probable as a shift of $-\frac{1}{2}a_{Si}$ (to the left), as expected from the mirror symmetry of the underlying Si(111) lattice. The same is true for k values of $\pm\frac{3}{2},\pm\frac{5}{2},\ldots$, etc. Our finding differs from Ref. 17 where different probabilities are found for positive and negative shifts, possibly due to insufficient statistics. Since we do not find any differences between $\pm k$, we take the sum $h(k)+h(-k)$ in Fig. 3 and plot it for positive k only.

It is worth mentioning that the statistical error bars for the interchain correlation $h(k)$ are larger than for the intrachain correlation $g(k)$ [compare Figs. 3 and 2(b)]. While the $g(k)$ have a Poisson distribution with an uncertainty equal to $\sqrt{g(k)/N_R}$, the uncertainty of the $h(k)$ is given by $\sqrt{h(k)\langle N_a\rangle/N_R}$, where $\langle N_a\rangle$ is the average number of atoms per chain uninterrupted by a domain wall or by the finite image size. For the set of data with optimum Au coverage $\langle N_a\rangle$ is 11.8. Since the number of dislocations for this surface is relatively small, the value of is dominated mostly by the total number of chains in all the STM images.

IV. MODEL HAMILTONIANS

The goal of the modeling is to reproduce, with rather few parameters, the spatial correlation function constructed from the STM images. In enumerating the sites, we use the surface lattice of the reconstructed surface as basis, which corresponds to a 5×2 cell of the truncated bulk structure. Therefore, the unit along the rows in the modeling is $2a_{Si}$, twice the spacing of the 5×1 cell used in Sec. III in the analysis of the images to include adatom pairs in different domains. That

is, the index $K=7$ in the modeling corresponds to $k=14$ in the images. As in a previous analysis,[17] the system is modeled as a lattice gas with strong nearest-neighbor repulsion J_1. With this parameter and a chemical potential μ set by the fractional coverage, the short-range correlations for $K=1-3$ are readily reproduced. The main new feature of the modeling is to introduce a rather long-range oscillatory interaction to fit the persistent correlations for $K=4-7$.

The main results of this work are obtained for the model Hamiltonian H:

$$H=\sum_i \sum_K J_K n_i n_{i+K} - \mu \sum_i n_i + H_1 \equiv H_0 + H_1 . \quad (1)$$

The occupation number n_i for site i has value 0 or 1 and J_1 and J_2 are the nearest-neighbor and next-nearest-neighbor interactions, at separations $2a_{Si}$ and $4a_{Si}$, respectively. The third term on the right-hand side represents a long-range substrate-mediated oscillatory interaction, perhaps arising from charge-density waves. It is a sum over adatom pairs:

$$H_1 = A \sum_{j<i} \cos(\pi[i-j]) \exp(-\epsilon|i-j|) n_i n_j , \quad (2)$$

where the damping factor with $\epsilon \rightarrow 0^+$ is introduced for convergence of the sums on an infinite chain.[24] The chemical potential term μ actually includes the interaction energy of one adatom with the substrate. A slight variant of H_0 is to introduce different site energies for the sites with even and odd index; the model then has two chemical potentials μ_1 and μ_2 and different average occupations $\overline{n_i}$ for even and odd i.

A second Hamiltonian with a simplified version of interchain interactions is defined for use in analyzing the interchain correlation in order to estimate the orders of magnitude of those interactions. Let there be adjacent chains α and β and retain strong nearest-neighbor intrachain repulsions J_1 and interactions J_2^{II} and J_3^{II} for the nearest-neighbors and next-nearest-neighbors between chains. Then H^{II} is

$$H^{II} = -\sum_i \mu[n_i(\alpha)+n_i(\beta)] + J_1 \sum_i [n_i(\alpha) n_{i+1}(\alpha) + n_i(\beta) n_{i+1}(\beta)] + J_2^{II} \sum_i n_i(\alpha) n_i(\beta) + J_3^{II} \sum_i [n_i(\alpha) n_{i+1}(\beta) + n_i(\beta) n_{i+1}(\alpha)]. \quad (3)$$

Thermal averages for Eq. (1) with $A=0$ and for Eq. (3) can be evaluated in a straightforward manner using transfer matrix techniques.[25] In fact, even the calculations for H^{II} reduce to manipulations with 4×4 matrices and thus most of the algebraic reduction is done analytically.

The effect of the long-range interaction H_1 is evaluated with first-order perturbation theory. The correlation function $g(K)$ for sites i,j separated by $K=|i-j|$ is defined, with thermal averages $\langle\cdots\rangle$ for Hamiltonian H,

$$g(K) = \langle n_i n_{i+K} \rangle / \langle n_i \rangle \langle n_{i+K} \rangle , \quad (4)$$

and the perturbation theory has, denoting thermal averages with H_0 by $\langle\cdots\rangle_0$,

$$\langle n_i \rangle \simeq \langle n_i \rangle_0 - \beta[\langle H_1 n_i \rangle_0 - \langle n_i \rangle_0 \langle H_1 \rangle_0], \quad (5)$$

$$\langle n_i n_{i+K} \rangle \simeq \langle n_i n_{i+K} \rangle_0 - \beta[\langle H_1 n_i n_{i+K} \rangle_0 - \langle n_i n_{i+K} \rangle_0 \langle H_1 \rangle_0]. \quad (6)$$

The correlation function can be given in quite explicit form for the nearest-neighbor case ($J_2=0$, $J_1 \equiv J$) of H_0. Then the eigenvalues of the transfer matrix are

$$\lambda_\pm = \tfrac{1}{2}[1+\exp\beta(\mu-J)] \pm \tfrac{1}{2}\sqrt{[1-\exp\beta(\mu-J)]^2 + 4\exp(\beta\mu}, \quad (7)$$

and the fractional occupation of a site is

$$\overline{n_0} = (1-\lambda_+)^2 \exp(-\beta\mu) / [1+(1-\lambda_+)^2 \exp(-\beta\mu)]. \quad (8)$$

Then, with $\Lambda \equiv \lambda_- / \lambda_+$, the correlation function is

$$g(K) = g_0(K) - \beta A g_1(K), \quad (9)$$

$$g_0(K) = 1 + \frac{(1-\overline{n_0})}{\overline{n_0}} \Lambda^K, \quad (10)$$

$$g_1(K) \simeq (-)^K (1-\overline{n_0})^2 (1-\Lambda)^2/(1+\Lambda)^2. \quad (11)$$

Equation (11) is the limiting behavior for large K and is accurate to 2% at $K>4$ for the parameters used in the present modeling. The calculations actually use the complete expression obtained from the first-order perturbation theory, Eq. (6), and extend from $K=1$ to $K=7$ ($k=2-14$ in the 5×1 units used in the analysis of the STM images).

V. INTERACTIONS IN A ONE-DIMENSIONAL LATTICE FLUID

Even before getting into quantitative models one can make a few qualitative observations about the relative sizes of the interactions governing the motion of the Si adatoms. There is a strong attraction of the extra Si atoms to the surface that immobilizes them at room temperature. From the mobility onset above[4] 500 K an activation energy of 1.2 eV has been estimated for diffusion along the rows.[18] The absence of any observed diffusion across the rows, even[4] at 800 K, shows the activation energy in that direction to be even larger (greater than about 2 eV). Of the adatom-adatom interactions, the largest term is a strong nearest-neighbor repulsion that almost completely excludes simultaneous occupation of the nearest-neighbor sites of the 5×2 lattice (Fig. 2). This is a conspicuous feature of the raw image data. The atoms missing from the nearest-neighbor separation $2a_{Si}$ seem to pile up at the next separation at $4a_{Si}$. Upon closer inspection of the image we can see extended chains of Si atoms with this spacing. Most of these chains contain 3–6 Si

atoms, but some have as many as 16, such as the one denoted by the arrow in Fig. 1(a). Such long chains, especially when numerous, are evidence for a long-range, intrachain interaction that enhances the values of $g(k)$ for $k=4m$, $m=1,2,3,\ldots$. In fact this effect is seen in Fig. 4 where the $g(k)$ at $k=4,8,12$ is at least 10% larger than the $g(k)$ at $k=6,10,14$. The weakest interaction is across the chains where we find a slight repulsion of the nearest neighbors. The barrier to motion between chains is so large and the correlation of positions of neighbor chains is so weak that we can focus our models exclusively on one-dimensional interactions along the chains.

We tested the ability of four models to reproduce the intrachain correlations, with parameters optimized by least-squares fits. These are (1) H_0 containing a nearest-neighbor repulsion J_1, (2) model 1 expanded by a second-neighbor interaction J_2, (3) model 1 with two site energies, and (4) model 1 with the nearest-neighbor repulsion augmented by an oscillatory coupling H_1. A fifth model using H^{II} introduces interchain correlations that might also mediate an effective longer-range intrachain correlation. Results for the two most successful models (1) and (4) are shown in Fig. 4.

Figure 4(a) shows that the first three experimental points can be fit very well by the theoretical correlation function for the nearest-neighbor repulsion model. For larger values of k ($k>6$, $K>3$), however, the calculated correlation very quickly approaches the random value of 1. The parameters μ and J_1 obtained from the fit are $-0.348k_BT$ (-21.0 meV for $T=700$ K) and $3.63k_BT$ (219 meV), respectively. They give $\overline{n_0}=0.248$, $\Lambda=-0.313$, and substitution in Eq. (10) shows explicitly the rapid decay. The exponential decay of the correlation is a general feature of one-dimensional models with short-range interactions, but we try other models to see whether minor changes would lead to correlations that persist beyond $k=6$.

Including a second-nearest-neighbor interaction J_2 in H_0 produces a fit which is almost identical to the nearest-neighbor result and therefore is not plotted. The parameters obtained are $\mu=-0.327k_BT(-19.7$ meV), $J_1=3.64k_BT$ (220 meV), and $J_2=0.000\,61k_BT$ (0.037 meV). The ratio $J_1/J_2=6000$ means that the second-nearest-neighbor interaction along the chain can be effectively neglected. The situation is similar for the model with interchain interactions, Eq. (3). With parameters $\mu=-0.290k_BT(-17.5$ meV), $J_1=3.63k_BT$ (219 meV), $J_2^{II}=0.213k_BT$ (12.9 meV), and $J_3^{II}=-0.010k_BT(-0.60$ meV), the fit to the experimental intrachain correlation function is visually undistinguishable from the one in Fig. 4(a) and therefore is not plotted. A more significant analysis is to use H^{II} to obtain the theoretical interchain correlation function. A least-squares fit to the experimental interchain correlation function $h(k)$ in Fig. 3 at $k=\frac{1}{2}, \frac{3}{2}$ gives an approximate value of the nearest-neighbor interchain repulsion $J_2^{II}=0.2k_BT$ (12 meV). Even with a large uncertainty of more than 25%, J_2^{II} is more than 10 times smaller than the intrachain repulsion J_1.

The persistence of correlations for $k=6-14$ can be reproduced in two ways. The first is to use H_0 with two types of adsorption sites. Then the least-squares fit gives $\mu_1=-0.268k_BT$, $\mu_2=-0.576k_BT$, and $J_1=3.43k_BT$. However, this leads[26] to significantly different average site occupations $\langle n_i\rangle_1=0.296$ and $\langle n_i\rangle_2=0.192$. This is not evident in the experimental STM images, and there is no other STM evidence for the existence of a 5×4 reconstruction with two inequivalent 5×2 sites.

The most viable model includes the oscillatory long-range term H_1 in the Hamiltonian and gives the good fit shown in Fig. 4(b). The theoretical correlation function does not approach 1 for higher k, but keeps oscillating around 1 with an amplitude of 0.05 through data with statistical uncertainty 0.03. For even values of $k<15$ plotted in Fig. 4(b), the theoretical correlation function matches quite well with the experiment. The parameters obtained are $\mu=-0.404k_BT$ (-24.4 meV), $J_1=3.59k_BT$ (217 meV), and $A=-0.0208k_BT(-1.26$ meV). That is, the parameters of H_0 are not much shifted and even the coherent energy effect of A for chains of ten atoms with spacing $4a_{Si}$ would be small compared to k_BT.

As discussed in Sec. III, for $k>15$ all even-indexed points of the experimental correlation function start to drop below the average value due to the defect induced domain boundaries. As shown in Fig. 2(b), the amount of this drop can be quantified by two solid fit lines drawn separately through the data points with even and odd k. If we add the values of the fit curve for odd k to the values of experimental correlation function for even k, the model correlation function maintains a rather good match with the experiment beyond $k=15$. However, this construction needs to be validated by a detailed analysis of domain boundaries and their effect on the system.

VI. SUMMARY

In summary, we have obtained high-quality Si(111)5×2 Au surfaces which consist of large domains with long, one-dimensional chains. Extra silicon atoms on top of the chains provide a well-controlled test bed for studying interactions in a one-dimensional lattice fluid. Five model Hamiltonians are developed for analyzing the high-statistics data on the correlations between the Si adatoms along and across the chains. The best description of the data is obtained by combining a strong nearest-neighbor repulsion with an oscillatory long-range interaction.

The interaction coefficients that are obtained in the modeling give information about the character of the adatom-adatom interactions along the chain. It is not a dipole repulsion, because that would give $J_2/J_1=1/8$ and the fit gave 1/6000. The scale of J_1 about 0.2 eV and the very short range of the repulsion are more consistent with a non-pair-additive interaction of two adatoms with a substrate in chemisorption.

While the nearest-neighbor repulsion might be expected for steric reasons, the necessity of including long-range oscillations is unusual. It might indicate an incipient reconstruction that would freeze in at lower temperatures if thermal equilibrium could be obtained. Actually, the presence of long-range commensurate $4\times$"2" charge density waves has been found on Si(111)4×1 In at low temperature,[27] and a

$c(4\times2)$ ordering of the dimer chains occurs on Si(100)2×1. Above the ordering temperature, a $c(4\times2)$ structure is still observed in the neighborhood of defects. For Si(111)5×2 Au we find that 5×2 reconstruction is better resolved next to the Si adatoms and becomes less sharp away from them [third row from the top in Fig. 1(b)]. This may be an indication that again a low-temperature reconstruction might be pinned by defects (Si adatoms) at high temperature. We have observed such an effect for a variety of chain structures induced by Au on stepped Si(111) surfaces. It would be interesting to pursue the role of electron or phonon instabilities in triggering long-range adatom correlations. For example, photoemission from this surface shows a nearly one-dimensional band structure near the Fermi level with a small electron pocket centered at $k=3/2\pi/a_{\mathrm{Si}}$.[16,28] Its diameter is consistent with a periodic instability at $4a_{\mathrm{Si}}$.

Correlations between surface atoms have a completely different relevance, too: The extra atoms on Si(111)5×2 Au have been used to build a prototype memory that stores 1 bit by the presence or absence of a single Si atom.[18] Such devices explore the atomic limit to density for storing data. The density limit is determined by the interaction between adjacent bits in this case, as well as in many other memory structures. Despite the fact that a bit was represented by a single atom, a unit cell of $5\times4=20$ atoms was required to keep the atoms spaced apart far enough to prevent interaction. As demonstrated by our correlation data, the smaller 5×2 unit cell would have suffered severely by the strong anticorrelation between adjacent 5×2 sites.

ACKNOWLEDGMENTS

The advice of S.N. Coppersmith, D.L. Huber, and M.B. Webb and experimental help from J.-L. Lin, J.N. Crain, and J.L. McChesney are gratefully acknowledged. This work was supported by the NSF under Grant Nos. DMR-9815416, DMR-0079983, and DMR-0104300.

*Permanent address: Department of Physics and Astronomy, University of Basel, 4056 Basel, Switzerland.

[1] H.J. Mikeska and M. Steiner, Adv. Phys. **40**, 191 (1991).
[2] M.W. Cole, V.H. Crespi, G. Stan, C. Ebner, J.M. Hartman, S. Moroni, and M. Boninsegni, Phys. Rev. Lett. **84**, 3883 (2000).
[3] M. Hodak and L.A. Girifalco, Phys. Rev. B **64**, 035407 (2001).
[4] T. Hasegawa and S. Hosoki, Phys. Rev. B **54**, 10 300 (1996).
[5] K. Amaya, H. Hori, I. Shiozaki, M. Date, M. Ishizuka, T. Sakakibara, T. Goto, N. Miura, K. Kikuchi, and Y. Ajiro, J. Neurophysiol. **59**, 1810 (1990).
[6] F.J. Himpsel, K.N. Altmann, R. Bennewitz, J.N. Crain, A. Kirakosian, J.L. Lin, and J.L. McChesney, J. Phys.: Condens. Matter **13**, 11 097 (2001).
[7] W. Swiech, E. Bauer, and M. Mundschau, Surf. Sci. **253**, 283 (1991).
[8] T. Hasegawa, K. Takata, S. Hosaka, and S. Hosoki, J. Vac. Sci. Technol. A **8**, 241 (1990).
[9] A.A. Baski, J. Nogami, and C.F. Quate, Phys. Rev. B **41**, 10 247 (1990).
[10] C. Schamper, W. Moritz, H. Schulz, R. Feidenhansl, M. Nielsen, F. Grey, and R.L. Johnson, Phys. Rev. B **43**, 12 130 (1991).
[11] J.D. O'Mahony, J.F. McGilp, C.F.J. Flipse, P. Weightman, and F.M. Leibsle, Phys. Rev. B **49**, 2527 (1994).
[12] L.D. Marks and R. Plass, Phys. Rev. Lett. **75**, 2172 (1995).
[13] L. Seehofer, S. Huhs, G. Falkenberg, and R.L. Johnson, Surf. Sci. **329**, 157 (1995).
[14] M. Shibata, I. Sumita, and M. Nakajima, Phys. Rev. B **57**, 1626 (1998).
[15] S.C. Erwin and H.H. Weitering, Phys. Rev. Lett. **81**, 2296 (1998).
[16] K.N. Altmann, J.N. Crain, A. Kirakosian, J.L. Lin, D.Y. Petrovykh, F.J. Himpsel, and R. Losio, Phys. Rev. B **64**, 035406 (2001).
[17] Y. Yagi, K. Kakitani, and A. Yoshimori, Surf. Sci. **356**, 47 (1996).
[18] R. Bennewitz, J.N. Crain, A. Kirakosian, J.-L. Lin, J.L. McChesney, D.Y. Petrovykh, and F.J. Himpsel, Nanotechnology **13**, 499 (2002).
[19] A. Kirakosian, J.N. Crain, J.L. Lin, J.L. McChesney, D.Y. Petrovykh, F.J. Himpsel, and R. Bennewitz, Surf. Sci. (to be published).
[20] R.P. Feynman in *The Pleasure of Finding Things Out*, edited by J. Robbins (Perseus, Cambridge, MA, 1999).
[21] J. Viernow, J.L. Lin, D.Y. Petrovykh, F.M. Leibsle, F.K. Men, and F.J. Himpsel, Appl. Phys. Lett. **72**, 948 (1998).
[22] R. Losio, K.N. Altmann, and F.J. Himpsel, Phys. Rev. Lett. **85**, 808 (2000).
[23] In the presence of domain boundaries, both even- and odd-numbered separations should become equally probable for large enough values of k. This means that fits to the occupancy of even- and odd-numbered separations should approach an asymptotic value of 0.5 corresponding to a random occupancy of the 5×1 lattice. The fact that fits for the Au-rich surface in Fig. 2(a) seem not to approach 0.5 for values of $k>40$ may be an artifact of the periodic boundary conditions used in obtaining the experimental pair distribution functions (see Sec. II).
[24] H_1 is intended to represent substrate-mediated interactions at intermediate separations and is used only as a perturbing term. There would be nonphysical pathologies if its effect were retained exactly in H.
[25] N. Goldenfeld, *Lectures on Phase Transitions and the Renormalization Group* (Addison-Wesley, Reading, 1992).
[26] The calculation was done with an average over adatom chains starting at the two types of sites, assuming these are present with Boltzmann factor weights but not resolved experimentally. The χ^2 of this fit is actually slightly better than that for the fit with H_1.
[27] H.W. Yeom, S. Takeda, E. Rotenberg, I. Matsuda, K. Horikoshi, J. Schaefer, C.M. Lee, S.D. Kevan, T. Ohta, T. Nagao, and S. Hasegawa, Phys. Rev. Lett. **82**, 4898 (1999).
[28] F.J. Himpsel, R.N. Altmann, J.N. Crain, A. Kirakosian, J.-L. Lin, A. Liebsch, and V.P. Zhukov, J. Electron Spectrosc. Relat. Phenom. **126**, 89 (2002); J.N. Crain *et al.* (unpublished).